Multiresolution Analysis on a spherical domain based on a flexible C^2 subdivision scheme over a valence 3 extraordinary vertex

Sara Grundel* Thomas P.Y. Yu †

April 22, 2010

Abstract:

It is known from a result of Prautzsch and Reif [19] that it is impossible to construct a flexible C^2 scheme over extraordinary vertices unless the regular subdivision scheme (assumed in [19] to be based on polynomial splines) is capable of producing polynomial patches of total degree 8 in the triangle case and bi-degree 6 in the quadrilateral case. Prautzsch-Reif's degree estimate, however, comes with a caveat, namely, that in the triangle mesh setting it is not applicable to the valence 3 case. In fact, the result in [19] is inconclusive about this valence 3 case. We show in this paper that, based on the 3-directional box-spline with directions $[1,0]$, $[0,1]$, $[1,1]$ repeated thrice, which produces degree 7 patches, it is actually possible to construct a flexible C^2 scheme over a valence 3 extraordinary vertex. Moreover, the characteristic map of this scheme coincides with a so-called valence 3 Bers' chart that shows up in the study of Riemann surfaces. As an application, this C^2 scheme gives rise to smooth hierarchical approximations of functions defined on a spherical domain.

In the quadrilateral case, Prautzsch and Reif's degree estimate applies to *all* valences greater than or equal to 3, suggesting that there is no chance of extending our result to quadrilateral meshes. Nonetheless, we discuss an unexpected extension to quadrilateral meshes.

Acknowledgments. We are grateful to Tom Duchamp and Hartmut Prautzsch for very helpful information directly related to the materials in this paper. We also acknowledge discussions with Pencho Petrushev and Qingtang Jiang on spherical multiresolution analysis. Yu is also grateful to a software donation by Alias. Finally, we thank Michael Overton for suggesting and supporting the collaboration.

1 Introduction

Subdivision surfaces are now a standard technique in free-form surface modeling and computer animation. From a technical viewpoint, a major breakthrough in the development of subdivision surfaces is the ability to handle the so-called extraordinary vertices. Since Euler characteristics

*Courant Institute of Mathematical Sciences, New York University. Email: grundel@courant.nyu.edu. She is supported in part by National Science Foundation Grant DMS 0714321.

†Department of Mathematics, Drexel University. Email: yut@drexel.edu. He is supported in part by National Science Foundation grants DMS 0512673 and DMS 0915068.

tell us that these extraordinary vertices can never be avoided in the arbitrary topology setting, the ability to construct well-behaved extraordinary vertex rules is the key to making subdivision surfaces applicable to the free-form setting. A mathematical theory for analyzing these extraordinary vertex rules has therefore been developed out of necessity; see, for example, [20, 28, 27, 16, 25] and the references therein.

The construction of flexible curvature continuous subdivision schemes over extraordinary vertices is a well-known difficult problem. It is beyond the scope of this paper to review all the attempts in attacking this problem; we mention only two early attempts [17, 22] and the most recent breakthrough [12]. It is known from a result of Prautzsch and Reif [19] that it is impossible to construct a flexible C^2 scheme over extraordinary vertices unless the regular subdivision scheme (assumed in [19] to be based on polynomial splines) is capable of producing polynomial patches of total degree 8 in the triangle case and bi-degree 6 in the quadrilateral case. Prautzsch-Reif's degree estimate, however, comes with a caveat, namely, that in the triangle mesh setting it is not applicable to the valence 3 case. In fact, the result in [19] is inconclusive about this valence 3 case.

Using a method called *jet subdivision*, it was shown that a C^2 scheme with the same subdivision stencils as the Loop scheme [11] actually exists in the valence 3 case, but the scheme requires the use of order 1 jet data and also it does not generate polynomial patches [26] for general control data. We show in this paper that it is actually possible to obtain a similar C^2 construction *without using jets*. Moreover, the scheme developed in this paper is based on a relatively simple 3-directional box-spline, instead of a non-interpolatory Hermite subdivision scheme [10] which does not generate piecewise polynomials.

Another contribution here is that our proof (Section 2) demystifies the flexible C^2 scheme constructed in [26], where some of the brute-force calculations that prove the desired C^2 condition seem rather un-insightful. Serendipitously, the proof technique in this paper also explains why Prautzsch-Reif's degree estimate does not hold in the valence 3 case.[1]

1.1 Practical motivations

Besides filling in a decade-old theoretical gap, another motivation for constructing such a smooth valence 3 scheme comes from the general interest in spherical wavelets [23, 14, 7, 13]. Note that a multiscale triangulation of a spherical domain can be constructed based on recursively subdividing a tetrahedron; such triangulations of the sphere consist only of valence 3 and 6 vertices. The subdivision scheme developed here gives rise to a smooth multiresolution analysis (MRA) on the topological sphere, which can potentially be used to construct biorthogonal wavelets on a spherical domain.

Such an MRA can also be directly used in finite element approximation of smoothing spline interpolation problems [5] on a genus 0 domain. In the case of the round sphere, the smoothing spline problem enjoys closed-formed expressions in its associated reproducing kernels [24], so there is no need for finite element approximation. However, in applications like geoid computation where one is interested in approximating a smooth function defined on a reference ellipsoid, the corresponding smoothing spline problem has no known closed formed solution and finite element methods become a natural approach.

Yet another motivation is the recent interest in numerical methods for conformal parametrization of genus 0 surfaces [8], which is based on the seminal work on harmonic mappings originated by

[1] In this connection, we thank H. Prautzsch for clarifying a key argument in [19].

Eells and Sampson [6]. It is perceivable that the smooth MRA on the sphere constructed in this paper can be used as a basis for the numerical computation of approximate conformal parametrization of genus 0 surfaces, or other kinds of finite element methods requiring hierarchical approximation of functions on a spherical domain.

With these potential applications in mind, we are prompted to consider an extension of the main result of this paper to the quadrilateral case. See Section 3.

1.2 Three directional box splines

Recall that a standard subdivision surface scheme is constructed based on a subdivision scheme in the regular grid setting followed by construction of special extraordinary vertex rules. In section 1.2, we discuss the specific regular subdivision scheme used in the construction in this paper. In Section 2, we show how a flexible C^2 scheme can be constructed in the valence 3 case.

The standard Loop scheme is based on the three directional box spline with directions $[1,0]$, $[0,1]$, $[1,1]$ each repeated twice. Recall the following definition of box-spline [18, 3]: Let $\Xi = \{v_1, v_2, \ldots, v_k\}$ be a set of k vectors in $\mathbb{R}^2$ with the first 2 vectors being linearly independent. The box-spline function B_Ξ is defined as follows. Let B_2 be the indicator function on the parallelogram $[v_1, v_2][0,1)^2$, scaled by the constant $1/\det[v_1, v_2]$, i.e. $B_2 := 1_{[v_1,v_2][0,1)^2}/\det[v_1, v_2]$. Then define $B_3, \ldots, B_k =: B_\Xi$ recursively by

$$B_\kappa(x) = \int_0^1 B_{\kappa-1}(x - tv_\kappa)\, dt, \quad \kappa > 2. \tag{1.1}$$

When the direction vectors have integral entries, the box spline $B_\Xi(x)$ can be generated by a dyadic subdivision scheme, which also means that it satisfies a refinement equation of the form $B_\Xi(x) = \sum_{\alpha\in\mathbb{Z}^2} a_\alpha B_\Xi(2x - \alpha)$.

In this paper we consider the three directional box spline with directions $[1,0]$, $[0,1]$, $[1,1]$ each repeated thrice. This box spline can be generated by a subdivision scheme whose mask $(a_\alpha)_\alpha$ has the following symbol (z-transform):

$$\sum_{\alpha\in\mathbb{Z}^2} a_\alpha z_1^{\alpha_1} z_2^{\alpha_2} =: \widehat{a}(z_1, z_2) = \frac{z_1^{-3} z_2^{-3}}{128}(1 + z_1)^3(1 + z_2)^3(1 + z_1 z_2)^3. \tag{1.2}$$

Since this scheme has the usual hexagonal symmetry of the regular triangular grid, it can be

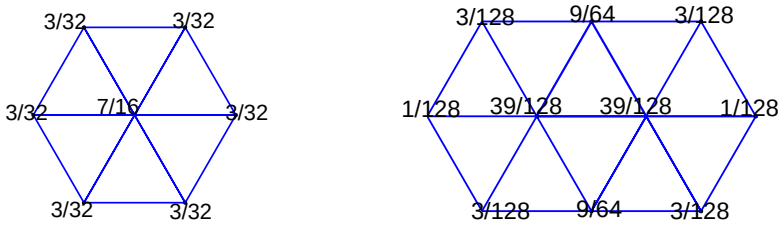

(a) vertex rule (b) edge rule, with a marquise-shaped stencil

Figure 1: Subdivision rules for the box spline with directions $[1,0]$,$[0,1]$,$[1,1]$ each repeated thrice.

used to construct subdivision surfaces in the arbitrary topology setting; the vertex and edge rules

associated with the mask (1.2) are shown in Figure 1. Notice that the vertex rule has the same stencil as that of the Loop scheme; the edge rule, however, has a bigger stencil compared to Loop's, but is still dependent only on the data in the 1-rings of the two end vertices of the edge.

Using standard sum rule conditions from subdivision theory, one can show that this subdivision scheme is the one and only one, among all the schemes with the same support, that reproduces all polynomials of total degree 4. In fact, this scheme also reproduces all polynomials of total degree 5. On the other hand, the box-spline function associated with (1.2) consists of degree 7 polynomial pieces (easy to see from (1.1), as each integration increases the degree by 1), and it is C^4 smooth.

2 Valence 3 Extraordinary Vertex Rules

In this section, we develop a valence 3 extraordinary vertex rule based on the regular rules in Figure 1. For this purpose, it suffices to work on the 3-regular complex, see Figure 3. Recall that the 3-regular complex has a central valence 3 extraordinary vertex with all other vertices being ordinary (valence 6). Away from the extraordinary vertex, our subdivision scheme uses the rules in Figure 1. In the vicinity of the valence 3 vertex, our proposed subdivision rules have the stencils, together with the weights labeled and to be determined, specified in Figure 2. The goal of this

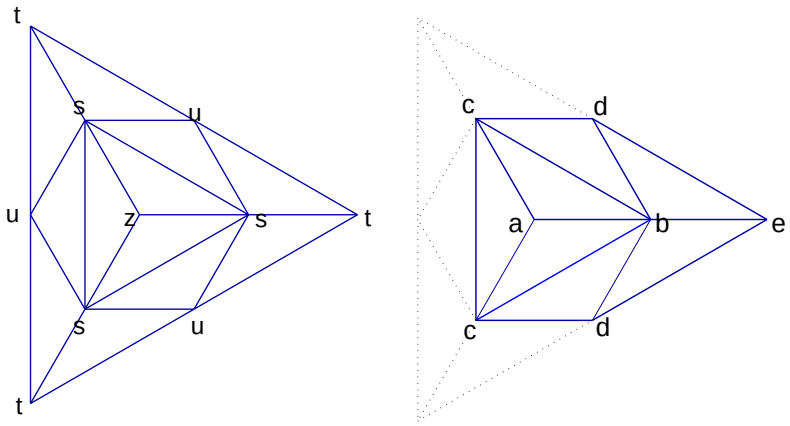

(a) extraordinary vertex rule $z = 1 - 3(s + t + u)$

(b) extraordinary edge rule $a = 1 - b - 2(c + d) - e$

Figure 2: Valence 3 extraordinary vertex rules. By the end of this paper, the weights will be chosen to be: $(z, s, t, u) = (31/128,\ 26/128,\ 1/128,\ 1/24)$ and $(a, b, c, d, e) = (17/64, 9/32, 3/16, 1/32, 1/64)$.

section is to determine a set of weights that give rise to a flexible C^2 scheme. Note that, according to Prautzsch-Reif's degree estimate [19], such a C^2 scheme is impossible for any valence greater than 3 other than 6.

We begin with some very well-known ideas in subdivision surface theory, and gradually move towards the relatively new observations.

2.1 Linear algebra

Like any other standard subdivision scheme, our scheme is **stationary**, meaning that the same set of rules is used at *all* levels. Together with the fact that these subdivision rules are linear, it is hardly surprising that eigendecomposition plays a key role in the analysis of subdivision schemes.

Given the support size of our proposed scheme, we need to use 3 rings of data around the extraordinary vertex in order to determine the subdivision limit function on the 1-disc (colored region in Figure 3(a)) around the extraordinary vertex. On the other hand, it is enough to use just 2 rings of data around the extraordinary vertex in order to determine the value of the limit function at the extraordinary vertex. Thus, the **subdivision matrix** of our scheme has the following block form

$$S = \begin{bmatrix} M & 0 \\ A & B \end{bmatrix} \tag{2.1}$$

if we order the vertices in the 3-regular complex as shown in Figure 3(a). Here,

$$M = \begin{bmatrix} z & s & s & s & t & u & t & u & t & u \\ a & b & c & c & e & d & 0 & 0 & 0 & d \\ a & c & b & c & 0 & d & e & d & 0 & 0 \\ a & c & c & b & 0 & 0 & 0 & d & e & d \\ 3/32 & 7/16 & 3/32 & 3/32 & 3/32 & 3/32 & 0 & 0 & 0 & 3/32 \\ 9/64 & 39/128 & 39/128 & 3/64 & 3/128 & 9/64 & 3/128 & 1/128 & 0 & 1/128 \\ 3/32 & 3/32 & 7/16 & 3/32 & 0 & 3/32 & 3/32 & 3/32 & 0 & 0 \\ 9/64 & 3/64 & 39/128 & 39/128 & 0 & 1/128 & 3/128 & 9/64 & 3/128 & 1/128 \\ 3/32 & 3/32 & 3/32 & 7/16 & 0 & 0 & 0 & 3/32 & 3/32 & 3/32 \\ 9/64 & 39/128 & 3/64 & 39/128 & 3/128 & 1/128 & 0 & 1/128 & 3/128 & 9/64 \end{bmatrix} \tag{2.2}$$

is the 10×10 matrix that maps the 2-ring data from one scale to the 2-ring data in the next finer scale, whereas the whole 19×19 matrix S maps the 3-ring data from one scale to the 3-ring data in the next scale. The entries in the blocks A and B come solely from the regular rules in Figure 1:

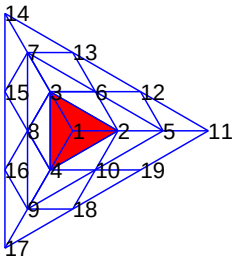

(a) Ordering of vertices
In red: the 1-disc around the e.v. (denoted by D)

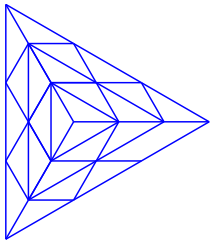

(b) Level 0 complex

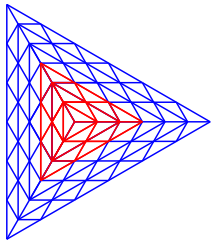

(c) Level 1 (once subdivided) complex

Figure 3: Ordering and subdivision of the 3-regular complex

$$A = \frac{1}{128}\begin{bmatrix} 1 & 39 & 3 & 3 & 39 & 18 & 0 & 0 & 0 & 18 \\ 3 & 39 & 18 & 1 & 18 & 39 & 3 & 0 & 0 & 3 \\ 3 & 18 & 39 & 1 & 3 & 39 & 18 & 3 & 0 & 0 \\ 1 & 3 & 39 & 3 & 0 & 18 & 39 & 18 & 0 & 0 \\ 3 & 1 & 39 & 18 & 0 & 3 & 18 & 39 & 3 & 0 \\ 3 & 1 & 18 & 39 & 0 & 0 & 3 & 39 & 18 & 3 \\ 1 & 3 & 3 & 39 & 0 & 0 & 0 & 18 & 39 & 18 \\ 3 & 18 & 1 & 39 & 3 & 0 & 0 & 3 & 18 & 39 \\ 3 & 39 & 1 & 18 & 18 & 3 & 0 & 0 & 3 & 39 \end{bmatrix}, \quad B = \frac{1}{128}\begin{bmatrix} 1 & 3 & 0 & 0 & 0 & 0 & 0 & 0 & 3 \\ 0 & 3 & 1 & 0 & 0 & 0 & 0 & 0 & 0 \\ 0 & 1 & 3 & 0 & 0 & 0 & 0 & 0 & 0 \\ 0 & 0 & 3 & 1 & 3 & 0 & 0 & 0 & 0 \\ 0 & 0 & 0 & 0 & 3 & 1 & 0 & 0 & 0 \\ 0 & 0 & 0 & 0 & 1 & 3 & 0 & 0 & 0 \\ 0 & 0 & 0 & 0 & 0 & 3 & 1 & 3 & 0 \\ 0 & 0 & 0 & 0 & 0 & 0 & 0 & 3 & 1 \\ 0 & 0 & 0 & 0 & 0 & 0 & 0 & 1 & 3 \end{bmatrix}.$$

The spectrum of S is the union of the spectra of M and B. The eigenvalues of the 9×9 matrix B are $1/32$, $1/64$, $1/128$ each repeated thrice. As we will see, the six dominant eigenvalues of S will be constructed to be $1, 1/4, 1/4, 1/16, 1/16, 1/16$, so these eigenvalues must come from the spectrum of M.

The rotational and reflectional symmetries of a subdivision scheme are necessary for applying it to the arbitrary topology setting. Rotational symmetry, alone, implies a block circulant structure in the subdivision matrix S and also the sub-matrix M. This, in turn, implies that M can be block-diagonalized by a suitable Fourier matrix.

One may not immediately see the block circulant structure in (2.2), but that is a just an artifact of the way we order the vertices: the ordering in Figure 2(a) is designed to give us the block structure in (2.1). To see the block circulant structure in M, simply reorder the vertices in the first two rings according to the following permutation:

$$\begin{pmatrix} 1 & 2 & 3 & 4 & 5 & 6 & 7 & 8 & 9 & 10 \\ 1 & 2 & 5 & 8 & 3 & 4 & 6 & 7 & 9 & 10 \end{pmatrix}. \tag{2.3}$$

If P is the corresponding row permutation matrix, then

$$\widetilde{M} := PMP^T = \begin{bmatrix} z & \mathbf{v}^T & \mathbf{v}^T & \mathbf{v}^T \\ \mathbf{w} & \mathbf{C}_0 & \mathbf{C}_1 & \mathbf{C}_2 \\ \mathbf{w} & \mathbf{C}_2 & \mathbf{C}_0 & \mathbf{C}_1 \\ \mathbf{w} & \mathbf{C}_1 & \mathbf{C}_2 & \mathbf{C}_0 \end{bmatrix} \tag{2.4}$$

where $\mathbf{v} = [s \;\; t \;\; u]^T$, $\mathbf{w} = [a \;\; 3/32 \;\; 9/64]^T$,

$$\mathbf{C}_0 = \begin{bmatrix} b & e & d \\ 7/16 & 3/32 & 3/32 \\ 39/128 & 3/128 & 9/64 \end{bmatrix}, \; \mathbf{C}_1 = \begin{bmatrix} c & 0 & 0 \\ 3/32 & 0 & 0 \\ 39/128 & 3/128 & 1/128 \end{bmatrix}, \; \mathbf{C}_2 = \begin{bmatrix} c & 0 & d \\ 3/32 & 0 & 3/32 \\ 3/128 & 0 & 1/128 \end{bmatrix}.$$

Now, $\widetilde{M}$ is still not block circulant as promised, but close. Let $\omega = \exp(-i2\pi/3)$, $\mathbb{I}$ be the 3×3 identity matrix, and $\mathbf{1} = [1 \;\; 1 \;\; 1]^T$. Then the circulant part of $\widetilde{M}$ is block diagonalized by

$$F = \begin{bmatrix} \mathbb{I} & \mathbb{I} & \mathbb{I} \\ \mathbb{I} & \omega\mathbb{I} & \omega^2\mathbb{I} \\ \mathbb{I} & \omega^2\mathbb{I} & \omega^4\mathbb{I} \end{bmatrix}, \quad \text{i.e. } F^{-1}\begin{bmatrix} \mathbf{C}_0 & \mathbf{C}_1 & \mathbf{C}_2 \\ \mathbf{C}_2 & \mathbf{C}_0 & \mathbf{C}_1 \\ \mathbf{C}_1 & \mathbf{C}_2 & \mathbf{C}_0 \end{bmatrix} F = \begin{bmatrix} \mathbf{B}_0 & & \\ & \mathbf{B}_1 & \\ & & \mathbf{B}_2 \end{bmatrix}, \tag{2.5}$$

for some 3×3 matrices $\mathbf{B}_i$; by computation,

$$\mathbf{B}_0 = \begin{bmatrix} b+2c & e & 2d \\ \frac{5}{8} & \frac{3}{32} & \frac{3}{16} \\ \frac{21}{32} & \frac{3}{64} & \frac{5}{32} \end{bmatrix}, \; \mathbf{B}_1 = \begin{bmatrix} b-c & e & \frac{d}{2} - \frac{\sqrt{3}d}{2}i \\ \frac{11}{32} & \frac{3}{32} & \frac{3}{64} - \frac{3\sqrt{3}}{64}i \\ \frac{33}{256} + \frac{33\sqrt{3}}{256}i & \frac{3}{256} + \frac{3\sqrt{3}}{256}i & \frac{17}{128} \end{bmatrix}, \; \mathbf{B}_2 = \overline{\mathbf{B}_1}. \tag{2.6}$$

With $z = 1-3(s+t+u)$ and $a = 1-b-2(c+d)-e$, each row of M sums to 1, meaning that $[1\ 1\cdots 1]^T$ is an eigenvector of M associated with the eigenvalue 1. This, together with $1+\omega+\omega^2 = 0$, implies that

$$\begin{bmatrix} z & \mathbf{v}^T & \mathbf{v}^T & \mathbf{v}^T \\ \mathbf{w} & \mathbf{C}_0 & \mathbf{C}_1 & \mathbf{C}_2 \\ \mathbf{w} & \mathbf{C}_2 & \mathbf{C}_0 & \mathbf{C}_1 \\ \mathbf{w} & \mathbf{C}_1 & \mathbf{C}_2 & \mathbf{C}_0 \end{bmatrix} \begin{bmatrix} 1 & 0 & 0 & 0 \\ \mathbf{1} & \mathbb{I} & \mathbb{I} & \mathbb{I} \\ \mathbf{1} & \mathbb{I} & \omega\mathbb{I} & \omega^2\mathbb{I} \\ \mathbf{1} & \mathbb{I} & \omega^2\mathbb{I} & \omega^4\mathbb{I} \end{bmatrix} = \begin{bmatrix} 1 & 0 & 0 & 0 \\ \mathbf{1} & \mathbb{I} & \mathbb{I} & \mathbb{I} \\ \mathbf{1} & \mathbb{I} & \omega\mathbb{I} & \omega^2\mathbb{I} \\ \mathbf{1} & \mathbb{I} & \omega^2\mathbb{I} & \omega^4\mathbb{I} \end{bmatrix} \begin{bmatrix} 1 & 3\mathbf{v}^T & & \\ 0 & \mathbf{B}_0 - 3\mathbf{e}\mathbf{v}^T & & \\ & & \mathbf{B}_1 & \\ & & & \mathbf{B}_2 \end{bmatrix}. \quad (2.7)$$

As such, we reduce M to a block diagonal matrix with one 4×4 and two 3×3 blocks. We refer to the 4×4 block as the 0-th block, and $\mathbf{B}_i$, $i = 1, 2$, as the i-th block.

We see immediately that 1 is an eigenvalue of the 0-th block. For convergence, it is necessary and sufficient that 1 is a simple eigenvalue. We denote the sub-dominant and sub-sub-dominant eigenvalues by λ and μ, so $1 > |\lambda| > |\mu|$.

An eigenvalue λ of M (and also of S) is said to have a **Fourier index** i if it 'comes from' (i.e. it is also an eigenvalue of) the i-th block. A multiple eigenvalue can have multiple Fourier indices. For simplicity, we assume that M will be constructed to have a real subdominant eigenvalue λ with geometric multiplicity 2 and a sub-sub-dominant eigenvalue $\mu = \lambda^2$ with geometric multiplicity 3; moreover,[2]

$$\mathcal{F}(\lambda) = \{1, 2\}, \quad \mathcal{F}(\lambda^2) = \{0, 1, 2\}. \quad (2.8)$$

Here $\mathcal{F}(\lambda)$ denotes the set of Fourier indices of the eigenvalue λ. We mention in passing that the first Fourier index condition is relevant to the injectivity of the characteristic map and the second is relevant to the curvature behavior in the vicinity of the extraordinary vertices; see [15, 16] for an in-depth theoretical development. While we do not need this part of the theory for our purpose, the above set of spectral conditions serves as a convenient guiding principle for our construction.

On the other hand, these spectral conditions alone are far from being sufficient for a scheme to be a flexible C^2 one. We recall the well-known C^1 and C^2 conditions in the next section.

2.2 Characteristic map and C^2 condition

Note that if $v \in \mathbb{R}^{19}$ is a set of scalar values assigned to the first 3 rings of the level 0 3-regular complex (as shown in Figure 3(a)), then according to our subdivision rules, the subdivision data on the first $2^j + 2$ rings of the level j 3-regular complex can be determined. Therefore, we obtain in the limit a subdivision function

$$f_v : D \to \mathbb{R}. \quad (2.9)$$

Here D is the 1-disc around the extraordinary vertex.

It is easy to see that every subdivision function satisfies the scaling relation

$$f_v(u) = f_{Sv}(2u), \quad \forall\, u \in \frac{1}{2}D. \quad (2.10)$$

In particular, if v is an eigenvector of S associated with an eigenvalue μ, then

$$f_v(u) = f_{\mu v}(2u) = \mu f_v(2u).$$

[2]These two conditions should be $\mathcal{F}(\lambda) = \{1, k-1\}$ and $\mathcal{F}(\lambda^2) = \{0, 2, k-2\}$ for a general valence k.

Despite the (rather artificial) way we embed D and the 3-regular complex into the plane as shown in Figure 3(a), one should not think of D as a subset of $\mathbb{R}^2$. That said, it is senseless to talk about the smoothness of f_v before we put a suitable differentiable structure on D (in differential geometry terms) or, equivalently, before we suitably parameterize f_v. On the other hand, since our subdivision scheme is based on a C^4 smooth box-spline, any subdivision function f_v is C^4 in the interior of each sector of D (assuming f_v is parameterized by the affine coordinates within each of the triangular sectors of D.)

The standard way to parameterize subdivision functions is based on *characteristic maps*, due to Reif [20]. Assume that we have a subdivision scheme that satisfies the spectral properties around (2.8). Let u_1 and u_2 be two linearly independent eigenvectors associated with the sub-dominant eigenvalue λ. The characteristic map is given by

$$\chi = (f_{u_1}, f_{u_2}) : D \to \mathbb{R}^2. \tag{2.11}$$

If χ is **injective**, we can think of $\chi^{-1} : \chi(D) \to D$ as a parametrization of D. If χ is also **regular**, i.e. χ has a non-singular Jacobian in the interior of each sector of D, then $f_v \circ \chi^{-1} : \chi(D) \to \mathbb{R}$ is C^1 smooth.

If we have a subdivision schemes that satisfies all the conditions above, except that all the eigenvalues smaller than λ are *strictly smaller* than λ^2 in modulus, then it is quite easy to show that all $f_v \circ \chi^{-1}$ are C^2 smooth. Such schemes are also easy to construct; the only problem is that they are not so useful since they produce limit functions with vanishing second derivatives *regardless of the initial data*, and hence are not so interesting from an approximation or modeling point of view. A **flexible** C^2 scheme is one that is both C^2 and capable of producing all quadratic polynomials.

Going back to our original assumption that the sub-subdominant eigenvalue is exactly λ^2 with geometric multiplicity 3, let w_i, $i = 1, 2, 3$, be three linearly independent eigenvectors associated with λ^2. Then we have the following well-known result:

Theorem 2.1. Such a subdivision scheme is a flexible C^2 one if

$$\text{span}\{f_{w_i} \circ \chi^{-1}(x_1, x_2) : i = 1, 2, 3\} = \text{span}\{x_1^2, x_1 x_2, x_2^2\}. \tag{2.12}$$

This result is not specific to the valence 3 case. In fact, everything we have said so far is either directly applicable to or has a generalization to any valence $k \geqslant 3$.

The condition in Theorem 2.1 seems hard to satisfy and, as illustrated by Reif-Prautzsch's degree estimates [19, 21], is indeed hard to satisfy when $k > 3$. In the rest of this section, we show:

Proposition 2.2. The weights in Figure 2 can be chosen such that:

(I) The resulted characteristic map χ is the valence 3 Bers' chart [1, 4] (called "fractional power embedding" in the quadrilateral case [16, Page 50], in which $z \mapsto z^{6/k}$ (see below) is replaced by $z \mapsto z^{4/k}$.)

(II) The eigenfunctions corresponding to sub-sub-dominant eigenvalues satisfy the flexible C^2 condition (2.12).

2.3 Valence 3 Bers' chart

The valence k Bers' chart is a piecewise fractional power function: on the first sector of a k-gon it is given by the analytic map $z \mapsto z^{6/k}$, assuming that the first sector is affine transformed into the equilateral triangle bounded by $[0,0]$, $[1,0]$ and $[\cos(2\pi/3), \sin(2\pi/3)]$, followed by identifying this equilateral triangle with part of the complex plane. In the other $k-1$ sectors, the chart is defined by rotational symmetry. It is not hard to check that these charts endow a triangle mesh with a conformal structure.

There is something special about the $k = 3$ case. First of all, the only $k \neq 6$ (and $\geqslant 3$) that makes $6/k$ an integer is $k = 3$. Moreover, we can identify the 3-gon D with the 'projective regular hexagon', i.e. the regular hexagon with antipodal points identified, as shown in Figure 4(a)-(b). Then under this identification, the valence 3 Bers' chart is the **single** map $z \mapsto z^2$. This representation of the valence 3 Bers' chart will be very useful in Section 2.7.

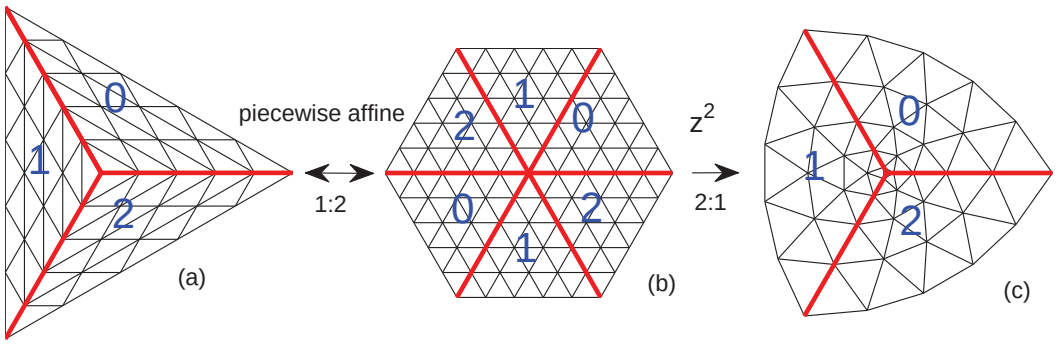

Figure 4: A general valence k Bers' chart is defined piecewisely. The valence 3 Bers' chart, however, can be expressed by the **single** polynomial $z \mapsto z^2$ if we identify the 3-gon D with the 'projective regular hexagon'.

2.4 Connection to Prautzsch-Reif's degree estimate

The valence 3 Bers' chart also gives a concrete illustration of how a key argument in Prautzsch-Reif's degree estimate breaks down in the valence 3 case. It is observed in [19] that if a valence k characteristic map consists of polynomial patches stitched together in a C^r fashion, and the polynomial pieces are only of degree r, then the characteristic map must be 6-periodic (see Lemma 5.1 and Theorem 5.1 of [19]), which is, in general, impossible as the characteristic map must also be k-periodic. (As a result, the polynomial degree must, in general, be $\geqslant r+1$; this lower bound is further improved to $\geqslant 3r/2+1$ by a finer argument.) The only exception is when $k = 3$, as illustrated by the valence 3 Bers' chart: it is both 3- and 6-periodic, and consists only of polynomial patches of degree 2 stitched together in a C^∞ fashion away from the extraordinary point.

2.5 Shaping the spectrum

Since

$$\chi\big(u/2\big) = \frac{1}{4}\chi(u), \quad \forall u \in D, \tag{2.13}$$

in order to have a chance to satisfy Property (I) above we must force our scheme to have a subdominant eigenvalue $\lambda = 1/4$. So, according to the spectral conditions around (2.8), we need $\mathbf{B}_0 - 3ev^T$ to have $1/16$ as a simple dominant eigenvalue, and $\mathbf{B}_1$, $\mathbf{B}_2$ both have $1/4$ and $1/16$ as simple dominant and sub-dominant eigenvalues.

$\mathbf{B}_0, \mathbf{B}_1, \mathbf{B}_2$ only involve the 4 parameters (b, c, d, e), but $\mathbf{B}_0 - 3\mathbf{e}[s \;\; t \;\; u]$ involves all 7 parameters (b, c, d, e, s, t, u). By (2.6), $\mathbf{B}_1$ and $\mathbf{B}_2$ already have $1/16$ as one of their eigenvalues. If we set

$$b = c - 3d - 4e + 1/4 \tag{2.14}$$

then $\mathbf{B}_1$, and hence also $\mathbf{B}_2$, both have $1/4$ as an eigenvalue; moreover, the corresponding two eigenvectors of M (which uniquely determine the corresponding eigenvectors of S due to the block form in (2.1)) are independent of the parameters:

$$\begin{aligned} u_1 &= \frac{1}{2}\Big[0,\ 2,\ -1,\ -1,\ 8,\ 3,\ -4,\ -6,\ -4,\ 3\Big]^T, \\ u_2 &= \frac{\sqrt{3}}{2}\Big[0,\ 0,\ 1,\ -1,\ 0,\ 3,\ 4,\ 0,\ -4,\ -3\Big]^T. \end{aligned} \tag{2.15}$$

Thanks to the Ferro-Tartaglia-Cardano's formula and modern symbolic computation, we find that by further setting

$$s = \frac{3/16 + 3(c - 2d - 5e + 8u + t) + 8(14dt + 6eu - 18ct + 24et - 3cu + 3du)}{3 - 16(d + 3e)}, \tag{2.16}$$

$\mathbf{B}_0 - 3ev^T$ has $1/16$ as an eigenvalue.

Therefore, after eliminating two of the seven parameters by (2.14) and (2.16), our subdivision matrix has the desired eigenvalues. As we shall see later, the C^2 condition specified by Theorem 2.1 will further take away two of the remaining 5 degrees of freedom, and then we have to choose the remaining 3 parameters in such a way that all the eigenvalues of M dependent of these parameters are $< 1/16$.

2.6 Relating valence 3 to valence 6

Everything in Section 2.1-2.2 is standard material. We now make an observation that is perhaps less standard.

Everything presented in Section 2.1-2.2 is also applicable to any valence $\geqslant 3$, and, in particular, to valence $k = 6$. Let N_r be the number of vertices in the first r rings of the 3-regular complex, so $2N_r - 1$ is the corresponding number for the 6-regular complex. Corresponding to (2.1), we have a size $2N_3 - 1 = 37$ subdivision matrix S_6 in the case of valence $k = 6$ in the following block form:

$$S_6 = \begin{bmatrix} M_6 & 0 \\ A_6 & B_6 \end{bmatrix}, \tag{2.17}$$

where all three blocks are determined by the regular rules in (1); M_6 is of size $2N_2 - 1 = 19$. (We order the vertices on the 6-regular complex in a way similar to Figure 3(a).) Corresponding to (2.9), we have $F_{\widetilde{v}} : H \to \mathbb{R}$ where $\widetilde{v} \in \mathbb{R}^{2N_3-1}$ is any set of data on the first three rings of the 6-regular complex, H is the 1-disc (a regular hexagon) around the central vertex, and $F_{\widetilde{v}}$ is the corresponding subdivision function.

Figure 4(a)-(b) suggests a 'doubling-up' operator from the 3-regular complex to the 6-regular complex; restricting this operator to the first r rings, we denote it by

$$\mathcal{D}_r : \mathbb{R}^{N_r} \to \mathbb{R}^{2N_r-1}.$$

The observation we need for proving Proposition 2.2 is the following:

Lemma 2.3. If $\widetilde{u} \in \mathbb{R}^{2N_3-1}$ is such that $F_{\widetilde{u}}$ is a homogeneous polynomial p of degree 2ℓ, then

1. $\widetilde{u}$ is an eigenvector of S_6 associated with eigenvalue $2^{-2\ell}$,
2. $\widetilde{u} \in \text{range}(\mathcal{D}_3)$, so $u := \mathcal{D}_3^{-1}\widetilde{u}$ is well-defined, and
3. $F_{\widetilde{u}}$, being an even function, can be viewed as a function on the projective regular hexagon $H/\!\sim$. (Here, $\mathbf{x} \sim \mathbf{y} \Leftrightarrow \mathbf{x} = \pm\mathbf{y}$.)

Furthermore, if (the parameters in M are chosen such that) $Su = 2^{-2\ell}u$, then

$$\mathbb{R} \leftarrow D : f_u = F_{\widetilde{u}} : H/\!\sim \to \mathbb{R} \tag{2.18}$$

if we identify D with $H/\!\sim$ (as in Figure 4.)

Sketch of proof. To appreciate the key idea in this lemma, first imagine that if we have an *arbitrary* vector $\widetilde{u}$ in range$(\mathcal{D}_3)$. We now subdivide $\widetilde{u}$ to the limit using the regular subdivision scheme operating on the 6-regular complex to get the limit function $F_{\widetilde{u}}$, and we subdivide $\mathcal{D}_3^{-1}\widetilde{u}$ to the limit using our subdivision scheme on the 3-regular complex to get f_u. Notice that the latter is based on a combination of the special valence 3 extraordinary vertex rule – used right at the vicinity of the valence 3 vertex – and the regular subdivision rule – used *away* from the valence 3 vertex, whereas the former has nothing whatsoever to do with any extraordinary vertex rule. Therefore, even though the regular subdivision scheme has the right symmetry to guarantee that $F_{\widetilde{u}}$ is an even function (since $\widetilde{u} \in \text{range}(\mathcal{D}_3)$), there is no reason to expect that $f_u = F_{\widetilde{u}}$.

However, under the assumption that $Su = 2^{-2\ell}u$ and $S_6\widetilde{u} = 2^{-2\ell}\widetilde{u}$, then, together with the natural symmetries of S and S_6, the extraordinary vertex rule and the regular subdivision scheme have essentially the same action in the vicinity of the corresponding central vertices; more precisely:

$$\mathcal{D}_3 S^j u = S_6^j \widetilde{u}, \quad \forall\, j = 0, 1, 2, \ldots$$

Away from the central vertices, both rules are based on the regular rule, so all together we have $f_u = F_{\widetilde{u}}$. ∎

Due to the block forms (2.1) and (2.17), to specify the vector $\widetilde{u}$ (resp. u) in the lemma above, it is enough to specify its first $2N_2 - 1$ (resp. N_2) entries. Call this shorter vector $\widetilde{u}^s$, if $\widetilde{u}^s \neq 0$, then $\widetilde{u}$ is uniquely determined by

$$\widetilde{u} = \begin{bmatrix} \widetilde{u}^s \\ (2^{-2\ell}I - B_6)^{-1}A_6\widetilde{u}^s \end{bmatrix}.$$

Notice that $\widetilde{u}^s \in \text{range}(\mathcal{D}_2)$. In the second half of the lemma above, we can actually weaken the assumption $Su = 2^{-2\ell}u$ to $M\mathcal{D}_2^{-1}\widetilde{u}^s = 2^{-2\ell}\mathcal{D}_2^{-1}\widetilde{u}^s$.

2.7 Proof of Proposition 2.2 and choice of parameters

We first prove Proposition 2.2(I) under only the condition (2.14). We shall only need condition (2.16) (and two new conditions on the parameters) when we deal with the C^2 conditions in Proposition 2.2(II).

The brute-force approach used in [26, Appendix B.7] can be applied here to prove (I). However, armed with Lemma 2.3, we can much more easily accomplish the task by checking that $\widetilde{u}_i := \mathcal{D}_2(u_i)$, $i = 1, 2$, are the (unique) data on the regular grid that generate the real and the imaginary parts of $z \mapsto z^2$ under the regular subdivision rule. Of course, the 6-regular grid, with coordinates denoted here by (x, y), can be identified with $\mathbb{Z}^2$, with coordinates denoted by (x_1, x_2), via a linear isomorphism:

$$\begin{bmatrix} x \\ y \end{bmatrix} = \begin{bmatrix} 1 & -1/2 \\ 0 & \sqrt{3}/2 \end{bmatrix} \begin{bmatrix} x_1 \\ x_2 \end{bmatrix},$$

so we are now back to the shift-invariant setting, and checking the polynomial reproduction condition above becomes a classical Strang-Fix-type calculation (a well-studied subject by itself.)

Using standard results in subdivision theory, any monomial of total degree $\leqslant 5$ can be written as a linear combination of the integer shifts of the three-directional box spline B_Ξ with subdivision mask (1.2). More precisely, if $\mu = (\mu_1, \mu_2)$, $|\mu| = \mu_1 + \mu_2 \leqslant 5$, then

$$x^\mu = \sum_{\alpha \in \mathbb{Z}^2} c_\alpha^\mu \, B_\Xi(x - \alpha), \tag{2.19}$$

where

$$c_\alpha^\mu = \sum_{\nu \leqslant \mu} \binom{\mu}{\nu} \alpha^\nu b_{\mu - \nu}, \tag{2.20}$$

and the b_μ, $|\mu| \leqslant 5$, are given by the following table[3]:

$\mu_1 \backslash \mu_2$	0	1	2	3	4	5
0	1	0	$-1/2$	0	$4/5$	0
1	0	$-1/4$	0	$2/5$	0	
2	$-1/2$	0	$2/5$	0		
3	0	$2/5$	0			
4	$4/5$	0				
5	0					

(2.21)

The real and imaginary parts of $z \mapsto z^2$ are

$$x^2 - y^2 = x_1^2 - x_1 x_2 - x_2^2/2, \quad 2xy = \sqrt{3}(x_1 x_2 - x_2^2/2). \tag{2.22}$$

Using (2.19)-(2.21),[4] it is straightforward to check that $\widetilde{u}_1$ and $\widetilde{u}_2$ are the unique vectors that generate these two degree 2 homogeneous polynomials on the x_1-x_2 plane. This verifies (I).

[3] These b_μ are computed recursively by the formula: $b_{(0,0)} = 1$, $b_\mu = \sum_{0 \neq \nu \leqslant \mu} \binom{\mu}{\nu} 2^{|\mu - \nu|} b_{\mu - \nu} [(-iD)^\nu \widehat{\mathbf{a}}](0)(1 - 2^{|\mu|}\widehat{\mathbf{a}}(0))^{-1}$, where $\widehat{\mathbf{a}}(\omega) = \sum_\alpha a(\alpha) e^{-i\alpha \cdot \omega}/4$. One can verify the values of b_μ in the table using this formula and (1.2).

[4] For a more elementary, but more tedious, approach, one can work out the piecewise (degree 7) polynomial representation of the box-spline B_Ξ based on (1.1) and use it to work out how to reproduce any polynomial of total degree $\leqslant 5$.

For (II) (the C^2 conditions), we need to force the sub-sub-dominant eigenvectors of M, w_i, $i = 1, 2, 3$, after 'doubling-up', to be the unique initial data that generate, under the regular subdivision rule, the following homogeneous degree 4 polynomials:

$$\begin{aligned}(x^2 - y^2)^2 &= x_1^4 - 2x_1^3x_2 + x_1x_2^3 + x_2^4/4,\\ (x^2 - y^2)(2xy) &= \sqrt{3}(x_1^3x_2 - 3x_1^2x_2^2/2 + x_2^4/4),\\ (2xy)^2 &= 3x_1^2x_2^2 - 3x_1x_2^3 + 3x_2^4/4.\end{aligned} \tag{2.23}$$

By calculations based on (2.19)-(2.21), we demand M in (2.1) to have the following three eigenvectors associated with eigenvalue 1/16:

$$\begin{aligned}w_1 &= \frac{1}{20}\Big[12,\ 2,\ -13,\ -13,\ 212,\ -33,\ -28,\ 102,\ -28,\ -33\Big]^T,\\ w_2 &= \frac{\sqrt{3}}{4}\Big[0,\ 0,\ -1,\ 1,\ 0,\ 9,\ -16,\ 0,\ 16,\ -9\Big]^T,\\ w_3 &= \frac{1}{20}\Big[12,\ -18,\ -3,\ -3,\ -108,\ 57,\ 132,\ -78,\ 132,\ 57\Big]^T.\end{aligned} \tag{2.24}$$

Condition (2.16) is only enough to guarantee that M has 1/16 as a triple eigenvalue, but not enough to guarantee the above eigenvector condition. After imposing conditions (2.14) and (2.16), M has 5 remaining parameters. After representing $M[w_1\ w_2\ w_3] - [w_1\ w_2\ w_3]/16$ in terms of these 5 parameters (c, d, e, t, u), we find that two extra linear conditions:

$$c = 9/64 + 3e, \quad d = 1/64 + e \tag{2.25}$$

are enough to guarantee that all entries in $M[w_1\ w_2\ w_3] - [w_1\ w_2\ w_3]/16$ are zeros.

Note that conditions (2.14) and (2.25) are linear but (2.16) is not. However, (2.25) and (2.16) together imply that $s = 3/16 + 2t$, so all the weights in our extraordinary vertex rule (Figure 2) are linearly dependent on the three parameters (e, t, u). This is bound to happen as the overall conditions imposed on M are, after all, linear:

$$M[u_1, u_2, w_1, w_2, w_3] = [u_1, u_2, w_1, w_2, w_3]\ \mathrm{diag}([1/4, 1/4, 1/16, 1/16, 1/16]).$$

We could have directly used the above to work out the same results; we just happened to go through the devious path of first working out conditions on the parameters *just* to satisfy the eigenvalue conditions (which are nonlinear and are of interests by themselves), before imposing the eigenvector conditions.

We must still verify that the remaining three parameters (e, t, u) can be chosen such that all the remaining eigenvalues are strictly less than 1/16 in modulus. This problem can be solved by a numerical search based on minimizing the largest of the remaining eigenvalues, a non-smooth non-convex eigenvalue optimization problem. We used the HANSO (Hybrid Algorithm for Non-Smooth Optimization) software package [2]; see [9] for a related application. For the specific problem at hand, only four eigenvalues of M are dependent on (e, t, u), and they are: $15/128 - 7e$ (repeated twice) and

$$\frac{1}{8} + e - \frac{9t}{2} - \frac{3u}{2} \pm \frac{1}{32}\sqrt{13 + 16(8e - 30t - 33u) + 256(4e^2 + 81t^2 + 9u^2 - 84et + 12eu + 54ut)}.$$

It can be shown analytically that these eigenvalues are smaller than 1/16 in modulus if and only if (e, t, u) lies in a small bounded open subset of the first octant of the e-t-u space. We recommend the following choice:

$$e = 1/64,\ t = 1/128,\ \ u = 1/24,$$

which give rise to the positive weights given in Figure 2. This choice is motivated by the usual convex hull property and the desire that the denominators in the weights possess as many dyadic factors as possible; the latter facilitates bitwise operations.

3 Extension to Quadrilateral Mesh

In the quadrilateral case, Prautzsch and Reif's degree estimate applies to *all* valences greater than or equal to 3, and there *seems* to be no chance to extend our result to quadrilateral meshes. But notice that the Bers' charts for the quadrilateral case (also known as "fractional power embedding" in [16]) is piecewise $z^{4/k}$ and when $k = 2$ we once again have a piecewise quadratic chart. Moreover, there is a description of this chart based on the **single** $z \mapsto z^2$ map analogous to the triangle case Figure 4; see Figure 6. This suggests that there is a chance to get around the degree estimate if we work with a valence 2 vertex.

Now, valence 2 vertex is almost unheard of in the subdivision community. For instance, nowhere in the recent monograph [16] or any publication we know is valence 2 vertex ever considered or even mentioned; the extraordinary vertex valence is always assumed to be at least 3 throughout all these publications. In personal communications with several subdivision researchers on this issue, the immediate response we got, with one voice, is that such valence 2 vertices represent a kind of 'degenerate situation', probably because the two quadrilaterals sharing a valence 2 vertex become 'degenerate quadrilaterals' as they look more like triangles than quadrilaterals (see, for example, Figure 7(d)-(e) below.)

Apparently, the existence of valence 2 vertices is not ignored by the developers of the commercial software Maya (`http://www.autodesk.com/maya`). In Figure 5, we generate a quadrilateral mesh for the topological sphere, with only valence 2 and valence 4 vertices, and subdivide it using the Catmull-Clark scheme implemented in Maya. While we do not know the details of the valence 2 rule in Maya (we will find our own below), the scheme appears to have a subdominant eigenvalue smaller than 1/2 and it appears to produce a reasonable limit surface. Based on the valence

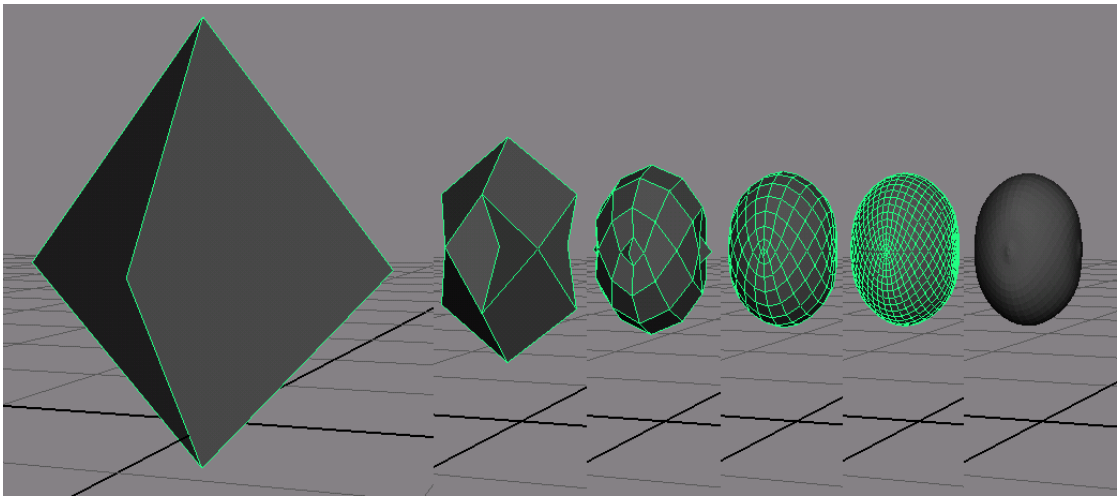

Figure 5: A quadrilateral mesh with valence 2 vertices, subdivided by Catmull-Clark scheme in the commerical software Maya. Thanks to Kyle McDonald for generating this picture in Maya.

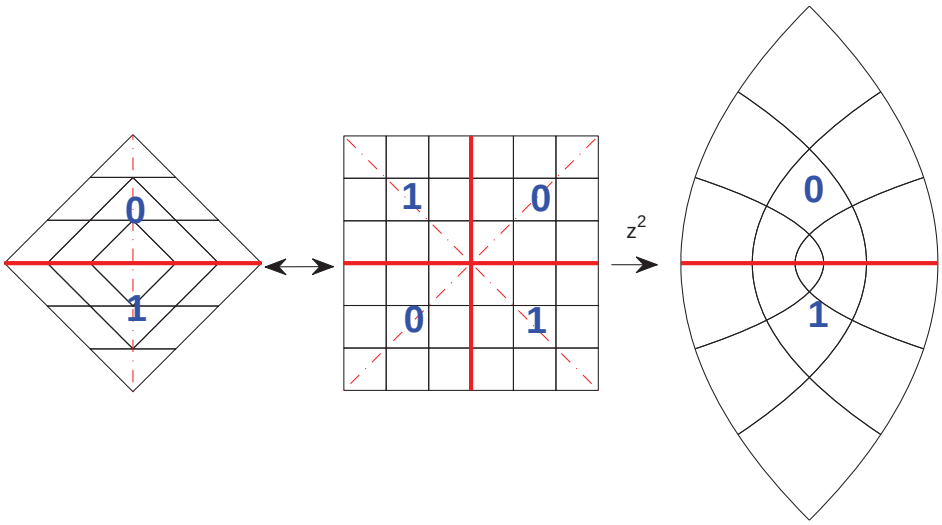

Figure 6: Valence 2 Ber's chart defined by the **single** polynomial $z \mapsto z^2$ when we identify the '2-regular complex' with the 'projective 4-regular complex', c.f. Figure 4.

2 Bers' chart shown in Figure 6, Lemma 2.3 (for relating valence 3 and valence 6 vertices in the triangle case) has an obvious extension to relate valence 2 and valence 4 vertices in the quadrilateral case. Based on the extended lemma, one can create a valence 2 extraordinary vertex rule for the Catmull-Clark scheme that has a characteristic map exactly equal to the chart in Figure 6. A possible solution is shown in Figure 7. Note that if we use the same stencils (but not necessarily the same weights) in Figure 7, the resulted valence 2 subdivision matrix for 1-ring data has the form:

$$\begin{bmatrix} 1-2(s_1+s_2) & s_1 & s_2 & s_1 & s_2 \\ 1-a-2b-d & a & b & d & b \\ 1/4 & 1/4 & 1/4 & 1/4 & 0 \\ 1-a-2b-d & d & b & a & b \\ 1/4 & 1/4 & 0 & 1/4 & 1/4 \end{bmatrix}.$$

Demanding the characteristic map to be the valence 2 Bers' chart is, then, according to the extended Lemma 2.3 and a corresponding Strang-Fix-type calculation, equivalent to demanding the above matrix to have $[0,1,0,-1,0]^T$ and $[0,0,2,0,-2]^T$ as eigenvectors associated with eigenvalue $1/4$ and all other eigenvalues except 1 to be smaller than $1/4$ in modulus. The eigenvector condition alone implies $a-d-1/4=0$ and poses no constraints on s_1 and s_2. All constraints are satisfied, for example, by (the non-unique choice) $(s_1, s_2, a, b, d) = (\frac{1}{16}, \frac{1}{8}, \frac{5}{16}, \frac{7}{64}, \frac{1}{16})$, which results in the scheme in Figure 7.

Such a valence 2 rule for the Catmull-Clark scheme, based on bi-cubic B-splines, is C^1 but not C^2. Using bi-quartic B-Splines, it is possible to create a flexible C^2 scheme. The details will be reported in a subsequent paper.

We reiterate that the study of these special C^2 schemes is motivated by their potential application in multiscale approximation of functions defined on a spherical domain. Valence 3 vertices in the triangle case and valence 2 vertices in the quadrilateral case are two key 'topological singularities' for a spherical domain.

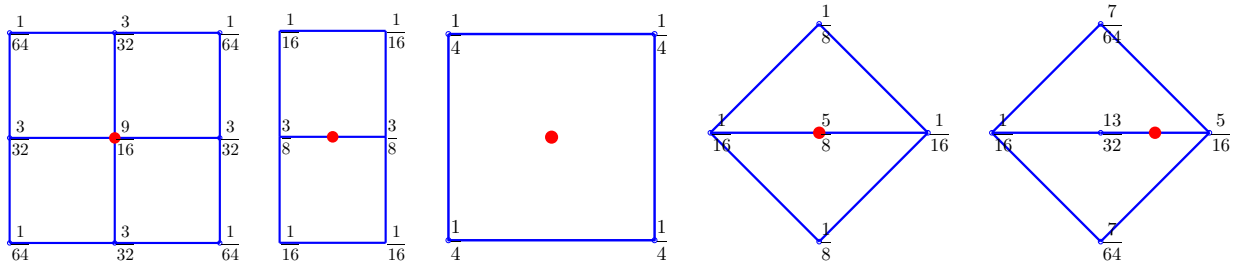

Figure 7: Valence 2 rule for the Catmull-Clark scheme: a)-c) vertex, edge and face subdivision rules for the standard bi-cublic B-spline used in the Catmull-Clark scheme, d) extraordinary vertex rule, e) extraordinary edge rule. The characteristic map of this scheme is the valence 2 chart shown in Figure 6. This scheme is C^1 but not C^2 smooth.

References

[1] L. Bers. *Riemann Surfaces*. Courant Institute of Mathematical Sciences, New York University, New York, 1958.

[2] J. V. Burke, A.S. Lewis, and M. L. Overton. *HANSO (hybrid algorithm for non-smooth optimization): a Matlab package based on BFGS, bundle and gradient sampling methods*. Version 1.0 released in 2006. See `http://www.cs.nyu.edu/faculty/overton/software/hanso/index.html`.

[3] C. de Boor, K. Höllig, and S. Riemenschneider. *Box Splines*. Springer-Verlag, 1993.

[4] T. Duchamp, A. Certain, A. DeRose, and W. Stuetzle. Hierarchical computation of PL harmonic embeddings. Preprint, July 1997.

[5] T. Duchamp and W. Stuetzle. Spline smoothing on surfaces. *Journal of Computational and Graphics Statistics*, 12(3):354–381, 2003.

[6] J. Eells, Jr. and J. H. Sampson. Harmonic mappings of Riemannian manifolds. *Amer. J. Math.*, 86:109–160, 1964.

[7] W. Freeden, T. Gervens, and M. Schreiner. *Constructive approximation on the sphere: with applications to geomathematics*. Numerical Mathematics and Scientific Computation. The Clarendon Press Oxford University Press, New York, 1998.

[8] X. Gu, Y. Wang, T. F. Chan, P. M. Thompson, and S-T. Yau. Genus zero surface conformal mapping and its application to brain surface mapping. *IEEE Transaction on Medical Imaging*, 23(8):949–958, 2004.

[9] B. Han, M. Overton, and T. P.-Y. Yu. Design of Hermite subdivision schemes aided by spectral radius optimization. *SIAM Journal on Scientific Computing*, 25(2):643–656, 2003.

[10] B. Han, T. P.-Y. Yu, and Y. Xue. Non-interpolatory Hermite subdivision schemes. *Mathematics of Computation*, 74(251):1345–1367, 2005.

[11] C. T. Loop. Smooth subdivision surfaces based on triangles. Master's thesis, Department of Mathematics, University of Utah, 1987.

[12] A. Myles and J. Peters. Bi-3 C^2 polar subdivision. *ACM Transactions on Graphics*, 28(3), August 2009. Article 48.

[13] D. Nain, S. Haker, A. Bobick, and A. Tannenbaum. Multiscale 3-D shape representation and segmentation using spherical wavelets. *IEEE Transactions on Medical Imaging*, 26(4):598, 2007.

[14] F. J. Narcowich, P. Petrushev, and J. D. Ward. Localized tight frames on spheres. *SIAM J. Math. Anal.*, 38(2):574–594, 2006.

[15] J. Peters and U. Reif. Shape characterization of subdivision surfaces – basic principles. *Computer Aided Geometric Design*, 21(6):585–599, 2004.

[16] J. Peters and U. Reif. *Subdivision Surfaces*. Springer-Verlag, Berlin, Heidelberg, 2008.

[17] H. Prautzsch. Freeform splines. *Computer Aided Geometric Design*, 14(3):201–297, 1997.

[18] H. Prautzsch and W. Boehm. Box splines. In *Handbook of computer aided geometric design*, pages 255–282. North-Holland, Amsterdam, 2002.

[19] H. Prautzsch and U. Reif. Degree estimates for C^k-piecewise polynomial subdivision surfaces. *Advances in Computational Mathematics*, 10(2):209–217, 1999.

[20] U. Reif. A unified approach to subdivision algorithms near extraordinary points. *Computer Aided Geometric Design*, 12:153–174, 1995.

[21] U. Reif. A degree estimate for subdivision surfaces of higher regularity. *Proceedings of the American Mathematical Society*, 124(7):153–174, 1996.

[22] U. Reif. TURBS — topologically unresticted rational B-splines. *Constructive Approximation*, 14:57–77, 1998.

[23] P. Schröder and W. Sweldens. Spherical wavelets: Efficiently representing functions on the sphere. *Computer Graphics Proceedings (SIGGRAPH 95)*, pages 161–172, 1995.

[24] Grace Wahba. Spline interpolation and smoothing on the sphere. *SIAM J. Sci. Statist. Comput.*, 2(1):5–16, 1981.

[25] J. Warren and H. Weimer. *Subdivision Methods for Geometric Design: A Constructive Approach*. Morgan Kaufmann, 2001.

[26] Y. Xue, T. P.-Y. Yu, and T. Duchamp. Jet subdivision schemes on the k-regular complex. *Computer Aided Geometric Design*, 23(4):361–396, 2006.

[27] D. Zorin. A method for analysis of C^1-continuity of subdivision surfaces. *SIAM Journal on Numerical Analysis*, 37(5):1677–1708, 2000.

[28] D. Zorin. Smoothness of subdivision on irregular meshes. *Constructive Approximation*, 16(3):359–397, 2000.